Field-induced behaviors near the smectic-*A*–smectic-C_α* phase transition of an antiferroelectric liquid crystal

Valéry Bourny and Hiroshi Orihara
Department of Applied Physics, Graduate School of Engineering, Nagoya University, Furo-cho, Nagoya 464-8603, Japan
(Received 15 June 2000; published 18 January 2001)

We have experimentally and theoretically investigated the electric-field effect on the smectic-*A*–smectic-C_α* phase transition of an antiferroelectric liquid crystal4-(1-methyl-heptyloxycarbonyl)phenyl 4′-octylcarbonyloxybiphenil-4-carboxylate. From the microscopic observations under electric fields and the measurements of the *D*-*E* hysteresis loop and apparent tilt angle, the *E* (electric field)-*T* (temperature) phase diagram was established, in which a tricritical point was found. From the dielectric measurements under dc electric fields, a soft mode inducing the transition was observed. Furthermore, we have developed a phenomenological theory under dc fields to analyze the experimental results. The origin of the soft mode observed under fields was clarified and the temperature dependence of the relaxation frequency was obtained by the analyses.

DOI: 10.1103/PhysRevE.63.021703 PACS number(s): 64.70.Md, 61.30.Gd, 64.60.Kw, 77.84.−s

I. INTRODUCTION

Subphases of antiferroelectric liquid crystals have been attracting much attention, among which the smectic-C_α*(SmC_α*) phase is especially of great interest. Its tilted character was clearly demonstrated by x-ray-diffraction experiments [1–3], and by optical measurements [4,5]. In addition, unusually large pretransitional tilt fluctuations have been reported in the vicinity of the Sm*A*-SmC_α* phase transition by heat capacity [6] and birefringence measurements [7]. The structure of the SmC_α* phase was recently determined to be incommensurate with the smectic layer [8] indicating that the soft mode should condense at a general point $\mathbf{q}_c$ of the smectic Brillouin zone. In actuality, we have recently succeeded in observing the soft mode in the SmC_α* phase [9]. All these results have definitively shown that the SmC_α* phase is brought about by the soft-mode condensation and the soft mode in the Sm*A* phase corresponds to a simple helix, and therefore the SmC_α* phase should also have a simple helix similar to the usual Sm*C**, but only different in pitch, as is expressed by the clock model [7].

On the other hand, also the electric-field effect on the Sm*A*-SmC_α* phase transition has been studied extensively by the measurements of the field-induced apparent tilt angle [10,11], optical transmittance [1,12], switching current responses [1,13,14], dielectric permittivity [11,14–17], and the conoscopic observations [2]. From some of these results it was found that the *antiferroelectriclike* behavior near the transition point to the Sm*A* phase changes to the *ferroelectriclike* or *ferrielectriclike* behavior in the low-temperature range of the SmC_α* phase. As for the antiferroelectric behavior, the double hysteresis loop was clearly observed in 11HFBBBM7 [14]. This result indicates that there should be a tricritical point in the *E* (electric field)-*T* (temperature) phase diagram because the order of the Sm*A*-SmC_α* phase transition changes from the second order under no field to the first order under fields. However, nothing has been reported about the tricritical point, though the *E*-*T* phase diagrams were made in methylheptyloxycarbonyl)phenyl 4′-octylbiphenyl-4-carboxylate (MHPOBC) [17] and 4-(1-methyl-heptyloxycarbonyl)phenyl 4′-octylcarbonyloxybiphenyl-4-carboxylate (MHPOCBC) [11]. On the other hand, from the dielectric measurements under dc electric fields, a few results related to the phase transition were reported [11,14–16]. Especially, in addition to the ferroelectric mode, a low-frequency mode was found in the low-temperature range of MHPOCBC [11]. However, there is no report in the high-temperature range close to the Sm*A*-SmC_α* phase-transition point.

In this paper, we focused our attention on the field-induced behaviors near the Sm*A*-SmC_α* phase-transition point, which may not be so complicated in comparison with those in the low-temperature range of SmC_α*. First, in order to confirm if there exists the tricritical point or not, we performed three independent measurements; the observation of texture evolution under fields and the measurements of apparent tilt angle and switching current. Next, the dielectric measurements under dc fields were made to show that there is an additional low-frequency mode also in the high-temperature range, which is the soft mode related to the Sm*A*-SmC_α* phase transition. Last, we present a simple phenomenological model that explains the experimentally obtained *E*-*T* phase diagram and the appearance of the soft mode under dc fields.

The paper is organized as follows. The experimental results are shown in Sec. II. Section III presents a simple theoretical description to explain the observed results. Section IV is devoted to conclusions.

II. EXPERIMENT AND RESULTS

The sample used was an antiferroelectric liquid crystal, 4-(1-methyl-heptyloxycarbonyl)phenyl 4'-octylcarbonyloxybiphenil-4-carboxylate (MHPOCBC). The phase sequence of MHPOCBC, on cooling given by differential scanning calorimetry (DSC) [18], is Iso.-(146.8 °C)-Sm*A*-(105.5 °C)-SmC_α* -(99.5 °C)-SmC_A* - (73.3 °C)-SmI_A*-(66.1 °C)-Cryst. The material was confined between two ITO (indium tin oxide)-coated glass slides, separated by

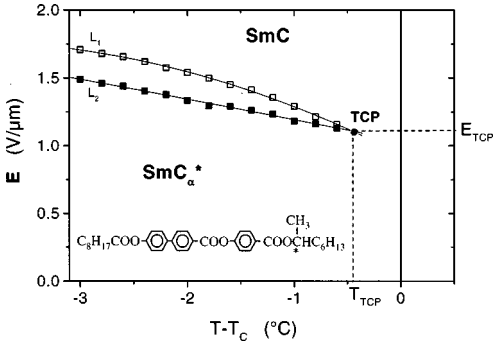

FIG. 1. Phase diagram of MHPOCBC constructed by the microscopic observation of texture change under dc electric fields.

spacers of 25 μm in thickness and the active area is 16 mm^2. To achieve a planar alignment, the glasses were covered with rubbed polyamide layers. The sample alignment was improved by applying a low-frequency ac electric field with thermal cycling around the Sm*A*-SmC_α* phase-transition point at a rate of 0.05 °C/min for 1 h.

The temperature was controlled by a hot stage (Instec HS-1) with an accuracy of ± 0.005 °C. The transition temperature from Sm*A* to SmC_α*, T_C, was determined carefully by the dielectric measurement. The transition temperature thus determined was slightly different from that by DSC measurements.

A. Texture observation under dc fields

The *E* (electric field)-*T* (temperature) phase diagram was constructed by the microscopic observation of texture change under dc electric fields, as shown in Fig. 1. We found a tricritical point (TCP) in the *E*-*T* phase diagram. Between T_{TCP} (the temperature of TCP) and T_C no texture change and no stripe were observed when the electric field was gradually increased, indicating that the direct transition from the SmC_α* phase to the unwound Sm*C* phase should take place continuously not through a structure with a large pitch. Below T_{TCP}, on the other hand, we observed the propagation of domains. When the electric field was increased, ferroelectric Sm*C* domains appeared and then propagated. Therefore, the field-induced transition from SmC_α* to Sm*C* is discontinuous with a typical hysteresis. The narrow region limited by the lines L_1 and L_2 in Fig. 1 corresponds to the coexisting state of them. The dc electric field could stabilize the coexisting state and some pictures of the texture were taken (see Fig. 2). It is clearly seen that the optical axis is different in the two domains. Near T_{TCP}, the optical contrast of these domains is weak [Fig. 2(a)], but far from T_{TCP} it becomes strong [Fig. 2(b)]. The domain boundaries are almost along the smectic layers.

In the subsequent subsections, we present the results of the apparent tilt angle and switching current measurements. The tricritical point is clearly observed also in these measurements.

B. Apparent tilt angle

The apparent tilt angle in planar geometry was measured as a function of the dc bias field by using the usual *optical 2θ method* [19]. Figure 3 shows the field dependences of the apparent tilt angle obtained at two typical temperatures. For $T_{TCP}<T<T_C$ [Fig. 3(a)], the continuous variation of the apparent tilt angle from the SmC_α* phase to the induced ferroelectric Sm*C* phase was observed. For $T<T_{TCP}$ [Fig. 3(b)], on the other hand, the variation of the apparent tilt angle became discontinuous. For small fields, the apparent tilt angle increased when the dc electric field was increased and at a critical value of electric field it jumped. Similar results were obtained by Hiraoka *et al.* in MHPOCBC [10] and in MHPOBC [11].

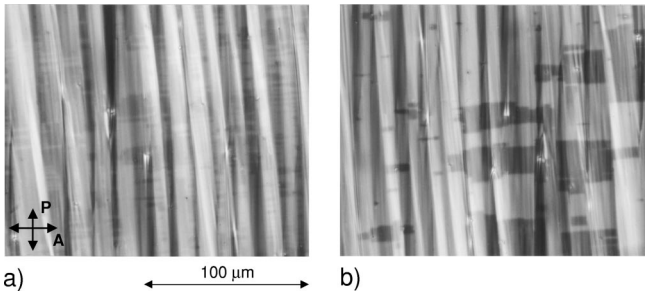

FIG. 2. The microphotographs of the texture in the SmC_α* phase under a dc electric field at (a) $T-T_C=-0.6$ °C, $E=1.15$ V/μm; (b) $T-T_C=-1.0$ °C, $E=1.25$ V/μm. The polarizers are crossed.

C. *D-E* hysteresis loop

D-E hysteresis loops were obtained by using the conventional method [20] with a triangular wave of 50 Hz. The switching current *I*, through a resistor connected with the sample, was measured with a digitizing oscilloscope and averaged over 200 periods.

We show two typical results of the switching current and the corresponding *D-E* hysteresis loop obtained by numerically integrating the current in Fig. 4. Two distinct behaviors were observed. For $T_{TCP}<T<T_C$ [Fig. 4(a)], the switching current is symmetric with respect to $E=0$ and no hysteresis is observed. For $T<T_{TCP}$ [Fig. 4(b)], on the other hand, the

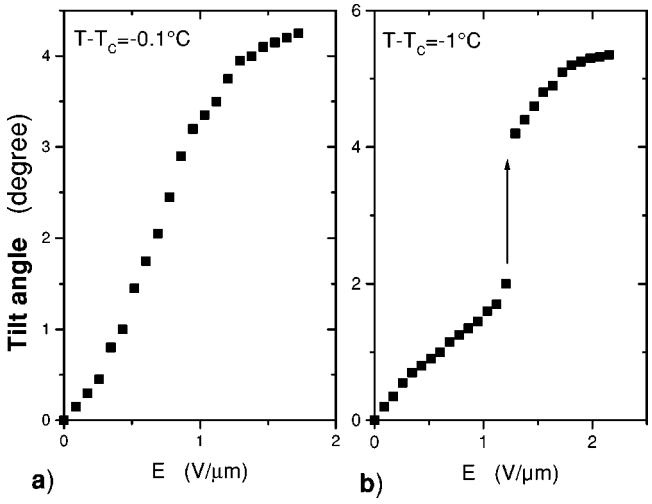

FIG. 3. Apparent tilt angle variation under dc field at (a) $T-T_C=-0.1$ °C, (b) $T-T_C=-1$ °C.

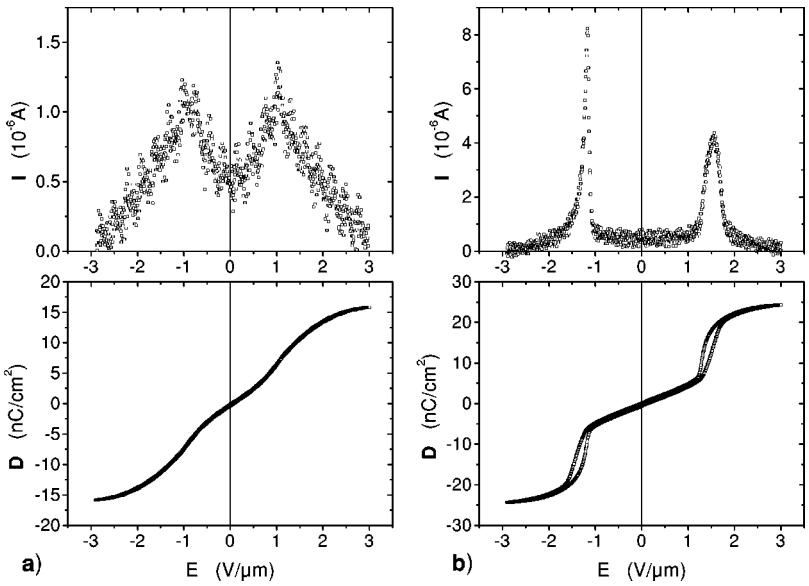

FIG. 4. Current peaks and the corresponding polarization hysteresis loops in the SmC_α^* phase at (a) $T-T_C=-0.2\,^\circ$C; (b) $T-T_C=-1.6\,^\circ$C.

switching current becomes asymmetrical and a double hysteresis loop appears. This result is also strong evidence exhibiting the existence of TCP.

The observation of the texture evolution in MHPOCBC under dc electric fields has shown the existence of a TCP on the *E-T* phase diagram, which was confirmed by the apparent tilt angle and switching current measurements.

D. Dielectric measurements under a dc field

The frequency dispersion of the complex permittivity was measured with an impedance analyzer (Hewlett Packard 4194A) in the frequency range of 100 Hz to 10 MHz. The ac probe field was 4.0 V/mm. The dielectric dispersion was measured as a function of temperature for different values of the dc bias field ($E=0$, 0.2, 0.4, 0.6, 0.8, 1, and 1.2 V/μm). According to the *E-T* phase diagram obtained experimentally in Fig. 1, $E_{\mathrm{TCP}}\approx 1.1\,\mathrm{V}/\mu\mathrm{m}$, and for $E<E_{\mathrm{TCP}}$ the transition from Sm*A* to SmC_α* is of second order, while for $E>E_{\mathrm{TCP}}$ it is of first order.

In Fig. 5, the real part of the dielectric constant, ε', at 100 Hz is presented for various dc bias fields. We can see that ε' has a maximum for all the dc fields and the peak value increases as the field is increased. However, it should be noted that the peak value at $1.2\,\mathrm{V}/\mu\mathrm{m}(>E_{\mathrm{TCP}})$ is still larger than those at 0.8 and $1\,\mathrm{V}/\mu\mathrm{m}(<E_{\mathrm{TCP}})$. By a microscopic observation it was found that the large peak is due to the coexistence of Sm*C* and SmC_α* and so not to the critical phenomenon. This is supported by the fact that ε' at $1.2\,\mathrm{V}/\mu\mathrm{m}$ $(>E_{\mathrm{TCP}})$ is smaller than those at 0.8 and $1\,\mathrm{V}/\mu\mathrm{m}\,(<E_{\mathrm{TCP}})$ in the Sm*A* phase.

In Fig. 6, typical frequency dispersions in the SmC_α* phase are shown. Without field [Fig. 6(a)] one mode is observed around 200 kHz, which is the ferroelectric mode. At $E=1\,\mathrm{V}/\mu\mathrm{m}$, on the other hand, another mode appears around 5 kHz [Fig. 6(b)]. This mode can be observed also at weaker fields, though the relaxation strength is small. The frequency dispersions were analyzed in terms of the Cole-Cole formula:

$$\epsilon(f)-\epsilon_\infty=\frac{1}{\left(i\dfrac{f}{f_c}\right)^{\delta}}+\sum_{j=1}^{n}\frac{\Delta\epsilon_j}{1+(jf/f_{r,j})^{\beta_j}}, \qquad (1)$$

where the first term accounts for the conductivity of the sample, ϵ_∞ is the dielectric constant at the high-frequency limit, and $f_{r,j}$, $\Delta\epsilon_j$, and β_j are, respectively, the relaxation frequency, the dielectric strength and the distribution parameter for the jth mode. The justification of Eq. (1) will be made in the next section. All the parameters are determined by the least-squares method. Typical results are shown in Figs. 7–9. Without field there is only the ferroelectric mode [$n=1$ in Eq. (1)], the relaxation strength and frequency show anomalies at the transition point [Figs. 7(a) and 7(b)], and β_1 decreases slightly in SmC_α* [Fig. 7(c)]. At 1 V/μm (Fig. 8), another mode was necessary for the fitting [$n=2$ in Eq. (1)]. From Fig. 8(a), it is found that this mode becomes soft as the transition point $T_C(E)$ is approached in the SmC_α* phase and the frequency becomes zero at $T_C(E)$, which is the

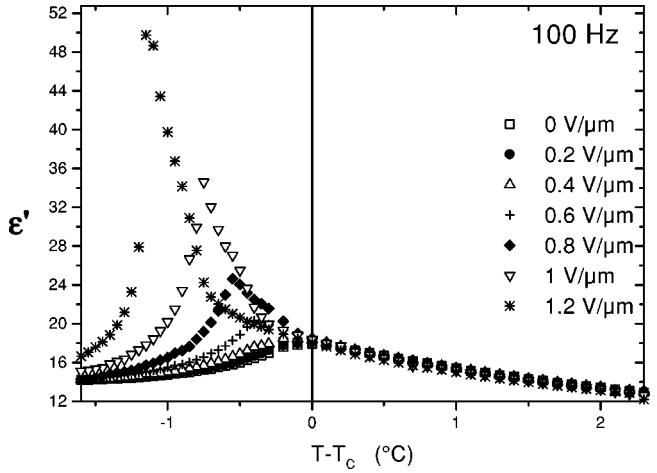

FIG. 5. Temperature dependences of the real part of the dielectric constant, ϵ', for different applied bias fields obtained at 100 Hz.

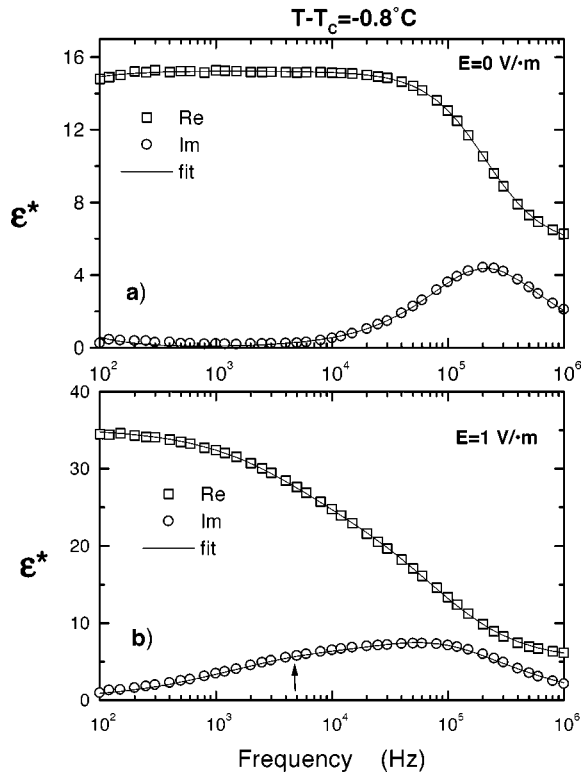

FIG. 6. Frequency dependences of the real and imaginary part of the dielectric constant ϵ^* at $T-T_C=-0.8\,^{\circ}\mathrm{C}$ under (a) no field and (b) $E=1\ \mathrm{V}/\mu\mathrm{m}$. Solid lines represent the best fit with Eq. (1).

field-induced phase-transition temperature between Sm*A* and SmC_α* phases. This behavior clearly indicates that this mode should be the soft mode related to the Sm*A*-SmC_α* phase transition. The relaxation strength increases near the transition point [Fig. 8(b)], which is one of the most remarkable characteristics. This soft mode has also been observed in the second-order electro-optic measurement without dc bias field [9]. Also in the Sm*A* phase there is a low-frequency mode, but this may not be the soft mode because its relaxation frequency is independent of temperature. In addition, in Fig. 8(c) the distribution factor β suddenly becomes small in the Sm*A* phase. This implies that these two modes should be different in physical origin. At $1.2\ \mathrm{V}/\mu\mathrm{m}\ (>E_{\mathrm{TCP}})$, where the transition is of first order, both the ferroelectric and soft modes show discontinuity in relaxation frequency at the transition point as shown in Fig. 9(a). The discontinuity is observed also in the relaxation strength [Fig. 9(b)] and the distribution factor β [Fig. 9(c)]. In Fig. 9(b), the steep increase of the low-frequency mode is especially noticeable, though the origin is not yet clarified.

III. THEORY

In this section, we will develop a Landau theory to describe the tricritical point and the appearance of the soft mode under a dc field. Here, we should notice the experimental fact that no stripe corresponding to the helical structure was observed with a polarizing microscope in the process of changing the applied field. This indicates that the

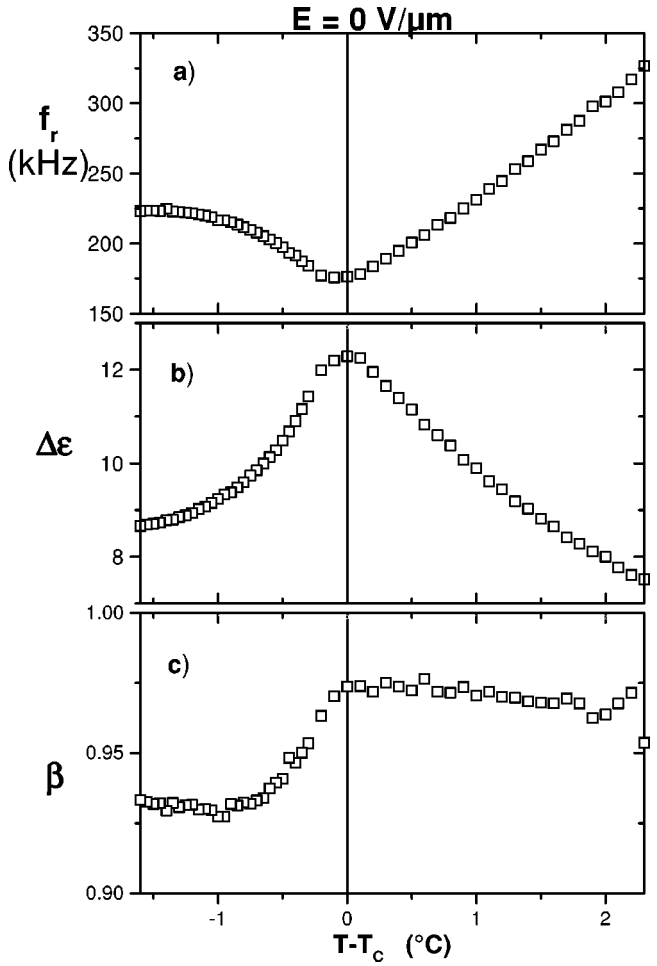

FIG. 7. Temperature dependences of (a) the relaxation frequency $f_{r,1}$, (b) the dielectric strength $\Delta\epsilon_1$, and (c) the distribution factor β_1 without bias field.

very-short-pitch helical structure in the SmC_α* should disappear without the divergence of the pitch, i.e., the amplitude of the helix should become zero. For this case we may express the order parameter in the jth layer as

$$\xi_{jx}=\xi_{fx}+\xi_q\cos q_c jd,$$
$$\xi_{jy}=\xi_{fy}+\xi_q\sin q_c jd, \tag{2}$$

where ξ_{fx} and ξ_{fy} are the ferroelectric order parameter, q_c is the wave number of the helix, ξ_q is the amplitude, and d is the layer spacing. We can regard q_c as constant, as mentioned above. When an electric field is applied along the x axis, the free-energy density f is given as

$$f=\tfrac{1}{2}\alpha_q\xi_q^2+\tfrac{1}{4}\beta_q\xi_q^4+\tfrac{1}{2}\alpha_f\xi_{fx}^2+\tfrac{1}{4}\beta_f\xi_{fx}^4 + \tfrac{1}{2}\eta\xi_q^2\xi_{fx}^2+\chi_f\lambda_f\xi_{fx}E_x-\tfrac{1}{4}\epsilon_a'\xi_q^2E_x^2, \tag{3}$$

where ϵ_a' is the dielectric anisotropy, χ_f is the dielectric susceptibility without the coupling between the polarization and the order parameter, and λ_f is the piezoelectric constant, by which the ferroelectric polarization, P_{fx}, is given as

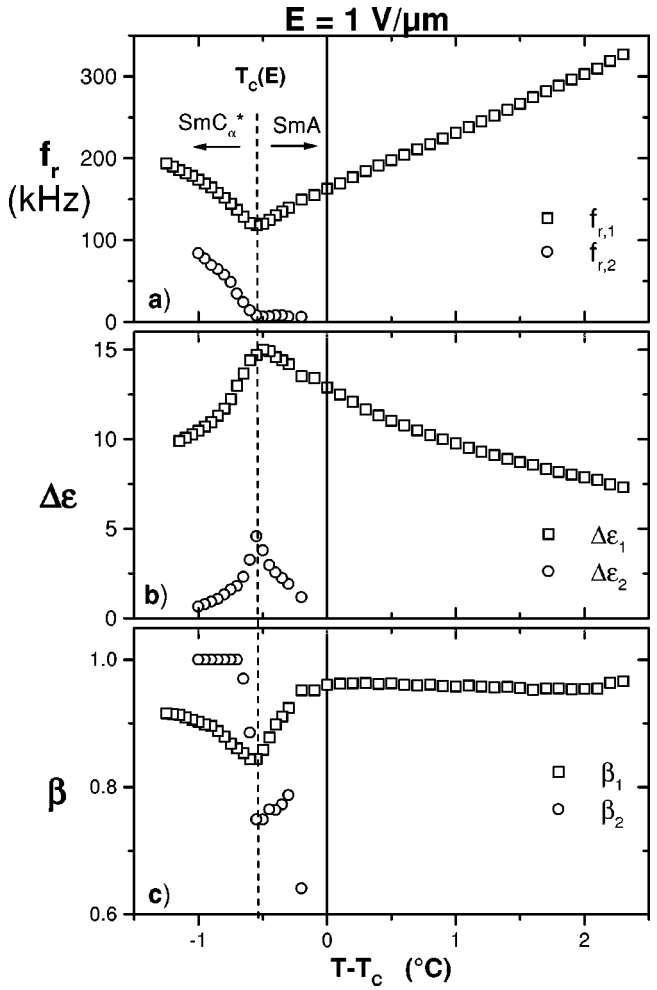

FIG. 8. Temperature dependences of (a) the relaxation frequencies $f_{r,i}$, (b) the dielectric strength $\Delta\epsilon_i$, and (c) the distribution factors β_i for the applied bias electric field $E=1$ V/μm.

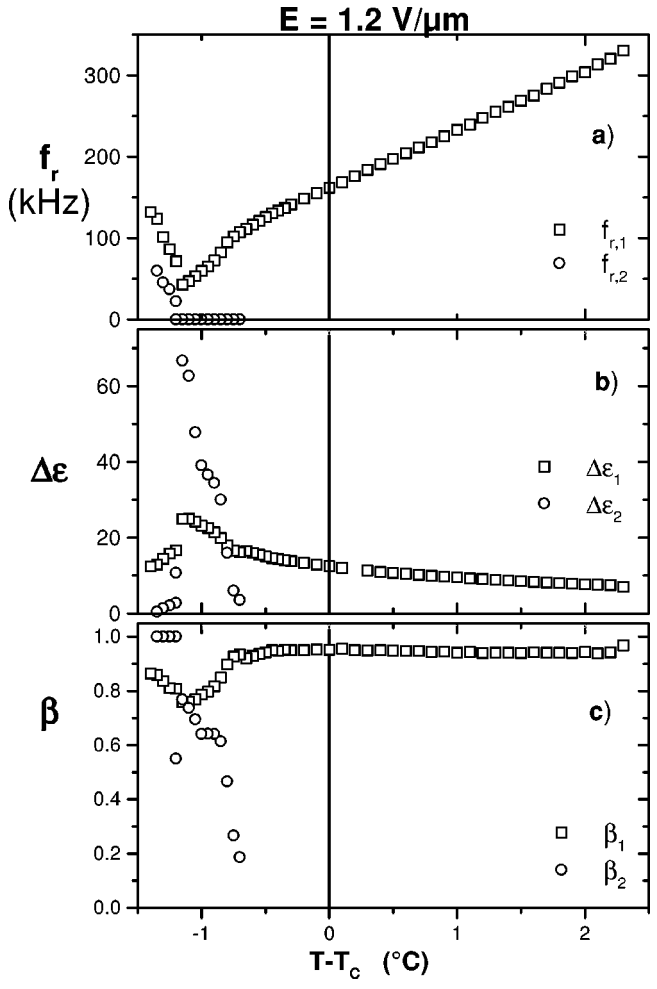

FIG. 9. Temperature dependences of (a) the relaxation frequencies $f_{r,i}$, (b) the dielectric strength $\Delta\epsilon_i$, and (c) the distribution factors β_i for the applied bias electric field $E=1.2$ V/μm.

$$P_{fx}=-\chi_f\lambda_f\xi_{fx}+\chi_f E_x. \tag{4}$$

The free-energy density without the last term in Eq. (3) has already been investigated in detail by Orihara and Ishibashi to explain the D-E double hysteresis loop observed in the SmC_A* phase [21]. The hysteresis loop may not be so changed when the dielectric anisotropy is introduced. However, the last term was shown to play an important role in the second-order electro-optic effect and the third-order dielectric response [22,9]. From the equilibrium conditions we get

$$\left(\alpha_f-\frac{\alpha_q\eta}{\beta_q}\right)\xi_{fx}+\left(\beta_f-\frac{\eta^2}{\beta_q}\right)\xi_{fx}^3+\chi_f\lambda_f E_x+\frac{\eta\epsilon_a}{2\beta_q}\xi_{fx}E_x^2=0 \quad \text{for Sm}C_\alpha^*, \tag{5}$$

$$\alpha_f\xi_{fx}+\beta_f\xi_{fx}^3+\chi_f\lambda_f E_x=0 \quad \text{for Sm}C, \tag{6}$$

giving the hysteresis loop. By assuming suitable temperature dependences of α_f and α_q and using the above equations and the following condition for the limit of stability,

$$\frac{\partial^2 f}{\partial\xi_{fx}^2}\frac{\partial^2 f}{\partial\xi_q^2}-\left(\frac{\partial^2 f}{\partial\xi_{fx}\partial\xi_q}\right)^2=0, \tag{7}$$

we can get TCP ($T_{\rm TCP}$,$E_{\rm TCP}$), where no hysteresis appears for $T_{\rm TCP}<T<T_C$ but it does for $T<T_{\rm TCP}$, as has been experimentally observed. A typical E-T phase diagram obtained by the present theory is shown in Fig. 10.

Next, we calculate the complex dielectric constant under a dc field E_0 by using the Landau-Khalatnikov equation of motion:

$$\gamma\frac{d\xi_q}{dt}=-\frac{\partial f}{\partial\xi_q},\qquad \gamma\frac{d\xi_{fx}}{dt}=-\frac{\partial f}{\partial\xi_{fx}}, \tag{8}$$

where γ is the rotational viscosity. When a small ac field ΔE is superimposed, i.e., $E_x=E_0+\Delta E$, the order parameters are also expressed as $\xi_q=\xi_{q0}+\Delta\xi_q$ and $\xi_{fx}=\xi_{f0}+\Delta\xi_f$, and the above equation becomes

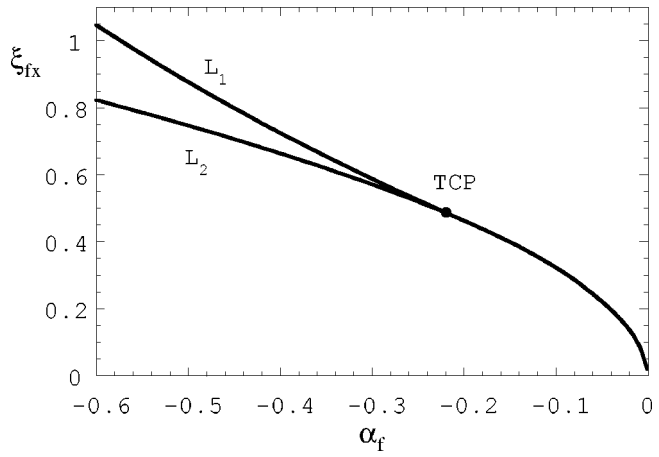

FIG. 10. Theoretically obtained phase diagram, where $\alpha_f=\alpha_q+1$, $\beta_q=0.3$, $\beta_f=\eta=1$, $\chi_f=1$, $\lambda_f=1$, and $\epsilon_a'=0.1$.

$$\gamma\frac{d\Delta\xi_q}{dt}=-(M_{11}\Delta\xi_q+M_{12}\Delta\xi_f)+e_1\Delta E,$$
$$\gamma\frac{d\Delta\xi_f}{dt}=-(M_{21}\Delta\xi_q+M_{22}\Delta\xi_f)+e_2\Delta E, \tag{9}$$

where $M_{11}=\partial^2 f/\partial\xi_{q0}^2$, $M_{12}=M_{21}=\partial^2 f/\partial\xi_{q0}\partial\xi_{f0}$, $M_{22}=\partial^2 f/\partial\xi_{f0}^2$, $e_1=-\partial^2 f/\partial\xi_{q0}E_0$, and $e_2=-\partial^2 f/\partial\xi_{f0}E_0$. By solving Eq. (9) for $\Delta E=\Delta E_0\cos\omega t$,

$$\Delta\xi_{q0}=\sum_{i=1}^{2}\frac{u_i(u_ie_1+v_ie_2)}{\lambda_i+i\omega\gamma}\Delta E_0,$$
$$\Delta\xi_{f0}=\sum_{i=1}^{2}\frac{v_i(u_ie_1+v_ie_2)}{\lambda_i+i\omega\gamma}\Delta E_0, \tag{10}$$

where $\Delta\xi_{q0}$ and $\Delta\xi_{f0}$ are the complex amplitudes of $\Delta\xi_q$ and $\Delta\xi_f$, respectively, λ_1 and λ_2 are the eigenvalues of the matrix M, and (u_1,v_1) and (u_2,v_2) are the corresponding eigenvectors. The piezoelectric coupling induces the polarization

$$\Delta P^{(s)}=-\chi_f\lambda_f\Delta\xi_{f0}+\chi_f\Delta E_0. \tag{11}$$

In addition to this, we have to take into account the field-induced dipoles of molecules. The dielectric constant along the x axis is

$$\epsilon_{xx}'=\epsilon_\perp'+\tfrac{1}{2}\epsilon_a'\xi_q^2, \tag{12}$$

where $\epsilon_\perp'$ is the dielectric constant perpendicular to molecules. Therefore, $(\epsilon_{xx}'-1)E_x$ yields

$$\Delta P^{(m)}=\epsilon_a'\xi_{q0}\Delta\xi_{q0}E_0-(\epsilon_\perp'-1+\tfrac{1}{2}\epsilon_a'\xi_{q0}^2)\Delta E_0. \tag{13}$$

Thus, we get the total dielectric susceptibility

$$\chi(\omega)=(\Delta P^{(s)}+\Delta P^{(m)})/\Delta E_0$$
$$=\sum_{i=1}^{2}\frac{(u_ie_1+v_ie_2)}{\lambda_i+i\omega\gamma}(-\chi_f\lambda_fv_i+\epsilon_a'\xi_{q0}E_0u_i)$$
$$+\chi_f+\epsilon_\perp'-1+\tfrac{1}{2}\epsilon_a'\xi_{q0}^2. \tag{14}$$

This result indicates that the dielectric dispersion under a dc field should consist of two Debye-type relaxations, as was experimentally shown. For small E_0, the above equation becomes

$$\chi(\omega)=\frac{1}{\lambda_1+i\omega\gamma}\left(\epsilon_a'-\frac{2\eta(\chi_f\lambda_f)^2}{\lambda_2(\lambda_2-\lambda_1)}\right)^2\xi_{qs}^2E_0^2$$
$$+\frac{1}{\lambda_2+i\omega\gamma}(\chi_f\lambda_f)^2+\chi_f+\epsilon_\perp'-1+\tfrac{1}{2}\epsilon_a'\xi_{qs}^2, \tag{15}$$

where $\lambda_1=2\beta_a\xi_{qs}^2$ and $\lambda_2=\alpha_f+\eta\xi_{qs}^2$ are the inverse susceptibilities of the soft mode and the ferroelectric mode, respectively. From the first term on the right-hand side of this equation, it is clear that the soft mode is observable by the dielectric measurement under a dc bias field and there are two different origins for the susceptibilities: the dielectric anisotropy and the coupling between the soft mode and the ferroelectric mode. In addition, it is worth noting that the first term is proportional to the squared field and so it is the third-order dielectric susceptibility, which is always positive. The physical meaning of the positive third-order susceptibility has been described in [22]. With increasing the field, the coupling constant between the soft mode and the ferroelectric mode, $M_{12}=2\eta\xi_{q0}\xi_{f0}$, increases so that the two modes should be mixed to make the two normal modes. As the tricritical point is approached in SmC_α*, λ_2 decreases and at the tricritical point it vanishes because $M_{11}M_{22}-M_{12}^2=0$ there. However, it should be noted that in the SmA phase, even if the tricritical point is approached it never vanishes. Therefore, there is discontinuity in dielectric susceptibility at T_{TCP}. Similarly, at the transition point between T_{TCP} and T_C under a bias field a jump appears at $\omega=0$, but not at $\omega>0$. In our experiments we could not observe the jump because the jump may be small and/or the measurements were done at finite frequencies.

IV. CONCLUSION

We have established the E-T phase diagram of MHPOCBC near the SmA-SmC_a* transition point and found a tricritical point. It was shown that the transition can be described by a model similar to the SmA-SmC_A* transition. The appearance of the soft mode induced by dc electric fields in the dielectric measurements was theoretically explained in terms of this model. There are two origins for it: one is the coupling between the soft mode and the ferroelectric mode, and the other is the dielectric anisotropy. The temperature dependence of the relaxation frequency was ob-

tained and it clearly showed the typical soft-mode character. In the dielectric measurements, on the other hand, a low-frequency mode was observed under fields near the transition point. The physical origin is not yet clear, but it may play an important role because the dielectric strength increases remarkably near the transition point. Therefore, it is necessary to develop a theory taking into account the coupling between the soft mode and the low-frequency mode.

ACKNOWLEDGMENTS

We would like to thank Showa Shell Sekiyu Co., Ltd. for supplying MHPOCBC. One of the authors (V.B.) thanks the Japan Society of Promotion of Science. This study was partly supported by a Grant-in-Aid from the Ministry of Education, Science, Sports and Culture (Grant No. 11099724 and No. 12650882).

[1] Y. Takanashi, K. Hiraoka, V. K. Agrawal, H. Takezoe, A. Fukuda, and M. Matsushita, Jpn. J. Appl. Phys., Part 1 **30**, 2023 (1991).

[2] T. Isozaki, K. Hiraoka, Y. Takanishi, H. Takezoe, A. Fukuda, Y. Suzuki, and I. Kawamura, Liq. Cryst. **12**, 59 (1992).

[3] P. Cluzeau, H. T. Nguyen, C. Destrade, N. Isaert, P. Barois, and A. Babeau, Mol. Cryst. Liq. Cryst. Sci. Technol., Sect. A **260**, 69 (1995).

[4] J. R. Lalanne, J. P. Marcerou, and G. Siguad, J. Phys. II **4**, 2149 (1994).

[5] I. Musevic, M. Skarabot, A. V. Kytik, R. Blinc, D. Moro, and G. Heppke, Ferroelectrics **203**, 133 (1993).

[6] K. Ema, M. Ogawa, A. Takagi, and H. Yao, Phys. Rev. E **54**, R25 (1996); K. Ema, A. Takagi, and H. Yao, *ibid.* **55**, 508 (1997); K. Ema and H. Yao, *ibid.* **57**, 6677 (1998).

[7] M. Skarabot, M. Cepic, B. Zeks, R. Blinc, G. Heppke, A. V. Kityk, and I. Musevic, Phys. Rev. E **58**, 575 (1998); M. Skarabot, K. Kocevar, R. Blinc, G. Heppke, and I. Musevic, *ibid.* **59**, R1323 (1999).

[8] P. Mach, R. Pindak, A. M. Levelut, P. Barois, H. T. Nguyen, C. C. Huang, and L. Furenlid, Phys. Rev. Lett. **81**, 1015 (1998).

[9] V. Bourny, H. Orihara, and A. Fajar, Phys. Rev. E **62**, R5903 (2000).

[10] K. Hiraoka, Y. Takanashi, H. Takezoe, A. Fukuda, T. Isozaki, Y. Suzuki, and I. Kawamura, Jpn. J. Appl. Phys., Part 1 **31**, 3394 (1992).

[11] K. Hiraoka, Y. Takanashi, K. Skarp, H. Takezoe, and A. Fukuda, Jpn. J. Appl. Phys., Part 2 **30**, L1819 (1991).

[12] T. Isozaki, Y. Suzuki, I. Kawamura, K. Mori, N. Yamamoto, Y. Yamada, H. Orihara, and Y. Ishibashi, Jpn. J. Appl. Phys., Part 2 **30**, L1573 (1991).

[13] P. Simeao Carvalho, M. R. Chaves, C. Desctrade, H. T. Nguyen, and M. Glagorova, Liq. Cryst. **21**, 31 (1996); P. Simeao Carvalho, M. Glagorova, M. R. Chaves, C. Desctrade, and H. T. Nguyen, *ibid.* **21**, 115 (1996).

[14] S. Sarmento, P. Simeao Carvalho, M. TR. Chaves, H. T. Nguyen, and F. Pinto, Mol. Cryst. Liq. Cryst. Sci. Technol., Sect. A **328**, 457 (1998).

[15] T. Sako, Y. Kimura, R. Hayakawa, N. Okabe, and Y. Suzuki, Jpn. J. Appl. Phys., Part 2 **35**, L114 (1996).

[16] R. Douali, C. Legrand, and H. T. Nguyen, Ferroelectrics **245**, 101 (2000).

[17] S. Tatemori, H. Uehara, J. Hatano, H. Saito, S. Saito, and E. Okabe, Jpn. J. Appl. Phys., Part 1 **38**, 5657 (1999).

[18] T. Isozaki, Y. Suzuki, I. Kawamura, K. Mori, N. Yamamoto, Y. Yamada, H. Orihara, and Y. Ishibashi, Jpn. J. Appl. Phys., Part 2 **30**, L1573 (1991).

[19] P. Martinot-Lagarde, R. Duke, and G. Durand, Mol. Cryst. Liq. Cryst. **75**, 249 (1981).

[20] P. Martinot-Lagarde, J. Phys. (France) Lett. **38**, L17 (1977); P. Martinot-Lagarde, Ferroelectrics **84**, 53 (1988).

[21] H. Orihara and Y. Ishibashi, Jpn. J. Appl. Phys., Part 2 **29**, L115 (1990).

[22] H. Orihara and Y. Ishibashi, J. Phys. Soc. Jpn. **64**, 3775 (1995).